Eur Biophys J (2007) 36:733–741
DOI 10.1007/s00249-007-0181-z

ORIGINAL PAPER

Effects of succinylation on thermal induced amyloid formation in Concanavalin A

Valeria Vetri · Fabio Librizzi · Valeria Militello · Maurizio Leone

Received: 21 December 2006 / Revised: 24 April 2007 / Accepted: 7 May 2007 / Published online: 7 June 2007

Abstract We have recently shown that upon slight thermal destabilization the legume lectin Concanavalin A may undergo two different aggregation processes, leading, respectively, to amyloid fibrils at high pH and amorphous aggregates at low pH. Here we present an experimental study on the amyloid aggregation of Succinyl Concanavalin A, which is a dimeric active variant of Concanavalin. The results show that, as for the native protein, the fibrillation process appears to be favoured by alkaline pH, far from the isoelectric point of the protein. Moreover, it strongly depends on temperature and requires large conformational changes both at secondary and tertiary structure level. With respect to the native protein, the succinyl derivative forms amyloid fibrils in considerably longer times and with a minor exposure of hydrophobic regions. At physiological conditions, Concanavalin A still displays a sizeable tendency to form amyloid fibril, while the succinyl variant does not. A close correlation was observed between the progress of amyloid formation and a narrowing of the tryptophans fluorescence emission band, indicating a reduction of protein conformational heterogeneity in amyloid fibrils.

Proceedings of the XVIII Congress of the Italian Society of Pure and Applied Biophysics (SIBPA), Palermo, Sicily, September 2006.

V. Vetri (✉) · F. Librizzi · V. Militello · M. Leone
Dipartimento di Scienze Fisiche e Astronomiche, Università di Palermo, Via Archirafi 36, 90123 Palermo, Italy
e-mail: valeria.vetri@fisica.unipa.it

V. Vetri · V. Militello · M. Leone
Consiglio Nazionale delle Ricerche, Istituto di Biofisica, Sez. di Palermo, Via U. La Malfa 153, 90146 Palermo, Italy

Keywords Concanavalin A · Succinylation · Protein aggregation · Amyloids · Fluorescence · Circular dichroism

Introduction

Concanavalin A (ConA) is an ''all-β'' protein belonging to the legume lectins family. It is a subject of interest for several scientific fields, ranging from the study of protein–carbohydrate interactions (Dam et al. 2000, 2002a, b; Mangold and Cloninger 2006), to protein folding (Sinha et al. 2005) and to medicine and physiology, where the protein is extensively used in model systems, due to its ability to induce liver injury (Tiegs et al. 1992; Ohta and Sitkovsky 2001; Song et al. 2003; Moreno et al. 2005; Fukuda et al. 2005).

ConA association state at quaternary level is governed by a reversible dimer–tetramer equilibrium, depending on pH and temperature: the protein is dimeric for pH values less than 6 and tetrameric at physiological conditions (Senear and Teller 1981; Bhattacharyya et al. 1991). The monomer (MW 26.000), whose tertiary structure has been described as a ''jelly roll'' motif (Mitra et al. 2002), presents a saccharide binding site and two metal binding sites, for Ca^{2+} and Mn^{2+}, respectively (Hardman et al. 1982; Sanders et al. 1998; Chatterjee and Mandal 2005), and is composed mainly of β structures, with no α helices. The absence of any disulphide bond enhances ConA flexibility, rendering it more prone to conformational changes at the tertiary structure level. The overall structure of the protein is reported to be remarkably similar to the structure of pentameric human serum amyloid P component, a protein which binds to all forms of amyloid fibrils and is universally found in amyloid deposits (Emsley et al. 1994). Interestingly, ConA was reported to induce programmed

cell death in cortical neurons, by a mechanism involving the cross-linking of cell surface receptors associated with the clustering of the inducing proteins on the surface (Cribbs et al. 1996).

Recently, we have shown that, in low-concentration regime and under slightly destabilizing conditions, ConA forms both fibrillar and amorphous aggregates in dependence of pH (Vetri et al. 2007). In particular, we observed amyloid formation at high pH (~9) and amorphous aggregation at pH 5, close to the isoelectric point (pI) of the protein.

Amyloids are generally insoluble, fibrous cross-β sheet protein aggregates. The process of amyloidogenesis occurs under conditions leading to partial unfolding of protein structure and is associated with several neurodegenerative pathologies such as Alzheimer's, Parkinson's and Huntington's disease (Harper and Lansbury 1997; Kelly 1998; Bellotti et al. 2000; Rochet and Lansbury 2000; Collinge 2001; Uversky and Fink 2004).

Here we study the aggregation pathways of Succinyl-ConA (S-ConA): this variant results from chemical derivatization of the tetrameric Concanavalin A with succinic anhydride. S-ConA retains several properties of the native Con A (Gunther et al. 1973; Waner et al. 1998; Edelman 1972). As a result of succinylation it is purely dimeric in solution and it does not re-aggregate to form tetramers at pH values above than 6 (Gunther et al. 1973). However in the crystalline form it was found as the typical Con A tetramer, thus suggesting the existence of a fine balance between dimer and tetramer (Moothoo et al. 1998; Fatima et al. 2006).

Succinyl-Con A is a widely used variant of Concanavalin A that seems to have unmodified carbohydrate binding properties but with altered biological activities (Gunter et al. 1973). The altered binding and biological activities of this derivative relative to tetrameric Con A have generally been attributed to their reduced valence. Moreover, it should be noted that succinylation most likely induces conformational constraints also at the tertiary structure level and has been reported to stabilize the protein and to reduce/prevent thermal aggregation at pH 5 (Fatima et al. 2006). Here we study amyloid fibrils formation of S-ConA at pH ~9 and at pH ~7.

Amyloid formation was monitored by means of Thioflavin T (TT) fluorescence (Naiki et al. 1989; Naiki and Gejyo 1999; Librizzi and Rischel 2005), which, as known, constitutes a selective probe for the detection of amyloid fibrils. Complementary information on the progress of the aggregation were obtained from the elastic scattering intensity of the fluorescence excitation beam. Protein conformational changes were investigated by means of 8-Anilino-1-Naphthalene-Sulfonate (ANS) fluorescence (Bauer et al. 2000; Vetri and Militello 2005), intrinsic tryptophans fluorescence (Lakovicz 1983; Militello et al. 2003) and far-UV Circular Dichroism (CD).

A comparison with the results obtained for the native protein shows that, even if the fibrillation process proceeds through analogous mechanisms, S-ConA is more stable and much less prone to aggregation. This is more evident at neutral pH and physiological temperature, where, contrary to the native protein, no amyloid formation was observed up to several days.

Experimental

Sample preparation

Succinyl-Concanavalin A (L3885), Concanavalin A (type IV L7647), ANS and (TT) were purchased from Sigma. All the measurements were performed in phosphate buffer 0.1 M at pH 8.9 and pH 7.2. Protein concentration was determined spectrophotometrically and was ~0.5 mg/ml (MW of Con A monomers: ~26,000). Every solution was freshly prepared and filtered just before the measurements through 0.22 μm filters. ANS and TT were dissolved in protein samples at concentrations of 24 and 13.3 μg/ml, respectively. Samples concentration, temperature and pH were selected as a good compromise to follow the aggregation processes of the two proteins in the same time interval.

Spectral measurements

Fluorescence spectra were carried out on Jasco FP-6500, equipped with a Jasco ETC-273T peltier as temperature controller. Samples were positioned in a 1 cm path cuvette and, after 3 min for thermal equilibration, emission spectra were recorded at 0.5 nm wavelength intervals.

For all samples, excitation spectra at 25°C, before and after each kinetics, were measured to monitor significant variations of the excitation band profile. The emission spectra of the intrinsic and extrinsic chromophores were obtained with emission and excitation bandwidth of 3 nm, scan-speed of 100 nm/min and integration time of 1 s, and recorded at 0.5 nm intervals. The measured spectral distributions A(E) were corrected for spectral response of the detection system (Lakovicz 1983).

The tryptophans emission spectra in the range 280–430 nm were obtained under excitation at 270 nm. ANS and TT emission spectra were detected using an excitation wavelength λ_{exc} = 380 and 440 nm, respectively.

Absorption measurements were carried out on a Jasco V-570 Spectrophotometer.

CD measurements were carried out on a Jasco J-715 spectropolarimeter, in the far-UV range using a 0.5 mm path quartz couvette and employing, as temperature controller, a Jasco PCT 348WI peltier. CD spectra were recorded sequentially, using a scan speed of 50 nm/min and a 1nm bandwidth; moreover, in order to follow the kinetics of spectra, no average of scans was employed.

CD and fluorescence measurements were made simultaneously, using different aliquots of the same freshly prepared sample.

Temperature Scan

Temperature Scan (T-Scan) of TT emission, including the elastic peak of excitation light at 440 nm were made on the Jasco FP-6500 spectrofluorimeter with the same parameters of kinetic measurements. Upward T-Scan were taken at 0.5°C intervals from 10 to 50°C, with a scan rate of about 12°C/h. At each temperature, complete emission spectra were taken to check out possible spectra variation upon heating at given temperature.

Since TT quantum yield depends on temperature, the obtained results were corrected by normalizing at each temperature for TT fluorescence in 76% glycerol-water solution.

Data analysis

It is well known that the intrinsic fluorescence emission spectra of proteins yield information about the local environment of the fluorophores in a protein and has found extensive application as a probe of protein structure and dynamics. In particular, the quantum yield and the position of the maximum of tryptophan fluorescence emission are solvent dependent; for example, a red-shift of the emission spectra indicates a more polar environment around the fluorophores (Lakovicz 1983; Vivian and Callis 2001; Militello et al. 2003). Moreover the broadening of the tryptophans emission bands gives information on protein conformational heterogeneity, since protein molecules in slightly different conformations may display slightly different emission wavelengths.

To obtain more quantitative information from the reported time evolution of tryptophans emission spectra (see Fig. 5 below) we analysed the momenta of the spectral distributions $A(E)$, where E is the emission energy. For each fluorescence spectrum, the zeroth (M_0), first (M_1) and second (M_2) momentum of the spectral distribution were calculated from the experimental data, after subtracting the tangent to the minima of each band, according to the following definitions:

$$M_0 = \int_{-\infty}^{\infty} A(E)\,\mathrm{d}E,$$

$$M_1 = \frac{\int_{-\infty}^{\infty} E \cdot A(E)\,\mathrm{d}E}{M_0},$$

$$M_2 = \frac{\int_{-\infty}^{\infty} E^2 \cdot A(E)\,\mathrm{d}E}{M_0} - M_1^2.$$

M_0 measures the integrated intensity, M_1 is the mean value of the emission energy and measures the position of the band and M_2 is the mean square deviation of the spectral distribution and measures its width.

Results

Figure 1a shows the elastic scattering intensity for S-ConA and ConA samples at pH 8.9 during upward T-Scans from 10 to 50°C (scan rate 12°C/h). For both samples, an increase in the scattering intensity is observed above a certain temperature (~20°C for ConA and ~40°C for S-ConA), thus indicating the onset of aggregation processes. In Fig. 1b, the simultaneously measured TT emission signal of both sample is presented. Data show a trend similar to the scattering intensity (Fig. 1a), although with less pronounced changes in the slope. Data clearly indicate for both samples the formation of amyloid fibrils, ConA being more prone to fibrillation than S-ConA. It should be noted that for ConA samples, at temperatures higher than 45°C, the formation of visible floccules occurs.

The observed data can be rationalized in terms of enhanced protein stability caused by derivatization of the tetrameric Concanavalin A with succinic anhydride. Succinylation, which converts positively charged amines into negatively charged carboxylates, leads to increased electrostatic repulsion (Chapman et al. 2003). The enhanced thermal stability of S-ConA with respect to ConA is probably brought about also by the structural constraints imposed by succinylation, which slightly alters the monomer conformation, partially preventing the conformational changes leading to aggregation.

In order to better characterize the aggregation process of S-ConA, we performed isothermal experiments by using different spectroscopic tools. Figure 2 shows the evolution of TT emission of S-ConA samples at pH 8.9, at four different temperatures as a function of time. To correct for the temperature dependence of the quantum yield of the dye, TT emission intensity was normalized to the constant value reached at the end of the aggregation kinetics. It should be noted that, once the samples were brought back to room temperature, the final values of TT emission were

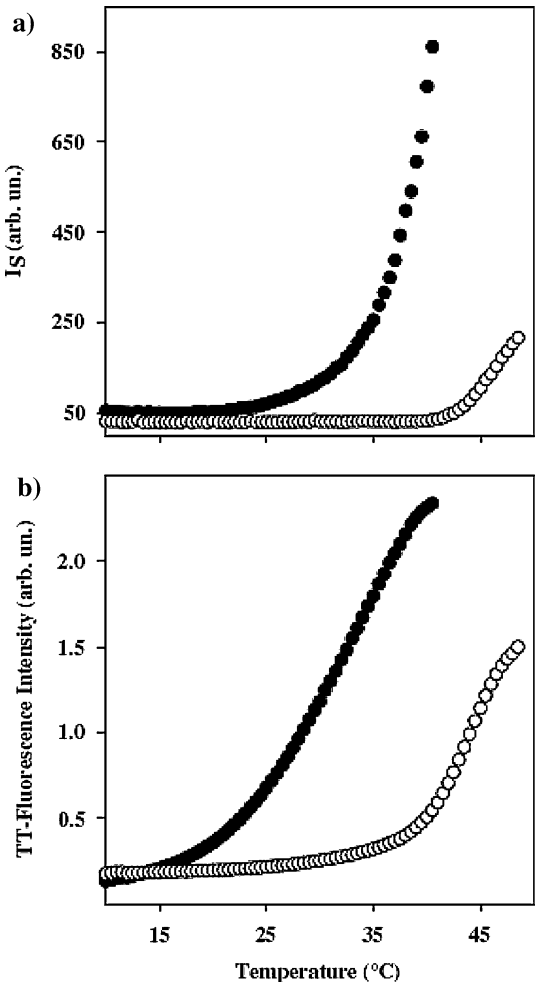

Fig. 1 **a** Elastic scattering intensity at $\lambda = 440$ nm, and **b** TT fluorescence emission (excitation wavelength 440 nm), as a function of temperature for ConA (*full symbols*) and S-ConA (*open symbols*). Both samples are at pH 8.9 and the scan rate is 12°C/h. Elastic scattering is measured on the excitation light of TT fluorescence, thus, data in the two panels are obtained in a single experiment

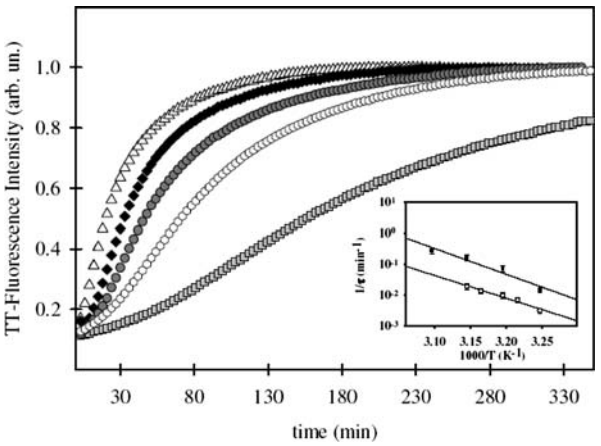

Fig. 2 TT fluorescence emission intensity as a function of time for S-Con A samples at pH 8.9 at five different temperatures (35°C *grey squares*, 37°C *white circles*, 40°C *dark grey circles*, 43°C *black diamonds* and 45°C *white triangles*). Data are normalized to the maximum value reached at the end of each kinetics. The inset shows an Arrhenius plot of the characteristic times for the fibrillation process in ConA and S-ConA. The parameter t is defined as the time necessary to reach 80% of the final fluorescence value

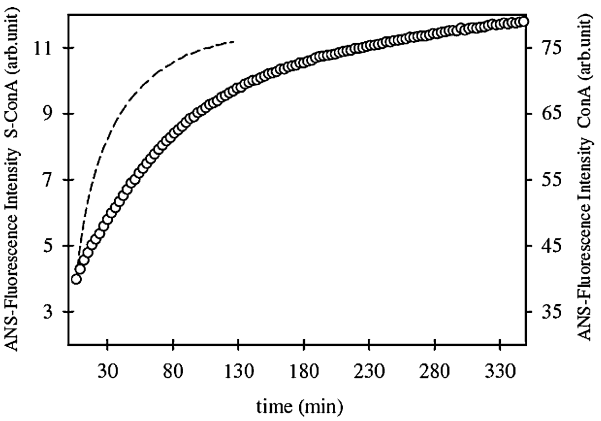

Fig. 3 ANS fluorescence emission as a function of time, for S-Con A (*left axis*) and ConA (*right axis*) (Vetri et al. 2007) at pH 8.9 and at 40°C. The excitation wavelength was at 380 nm

the same within the experimental errors. In the same conditions ConA fibrillation is much faster: for instance, at 40°C the kinetics of ConA samples reaches the maximum after ~40 min (Vetri et al. 2007), while S-ConA requires ~300 min.

This is also evidenced in the inset of Fig. 2, which shows an Arrhenius plot of the inverse characteristic times for the fibrillation process both in ConA and S-ConA. The kinetic parameter used for this analysis (τ) is defined as the time necessary to reach 80% of the final fluorescence time. Notwithstanding the very small temperature range, this plot allows us to estimate that the activation enthalpies of the fibrillation process (the slopes of the straight lines in the inset) are roughly the same for ConA and S-ConA. Therefore, data suggest that the in S-ConA the fibrillation process is slower than in ConA mainly for entropic reasons. This is somewhat surprising, since one could think that the most relevant effect of succinylation is an enthalpic stabilization of the protein.

Figure 3 shows the kinetic emission of ANS for a S-ConA sample at pH 8.9 and at 40°C. This probe is widely used to monitor changes involving hydrophobic regions already present in protein structures or formed during the evolution of the aggregation (Relini et al. 2004; Souillac et al. 2003; Morel et al. 2006). The enhancement of ANS fluorescence intensity indicates an increase of exposed hydrophobic regions, brought about by conformational changes, leading to a partial loss of tertiary structure. The kinetic emission of ANS for a ConA sample in the same conditions is reported for comparison (dashed line, right

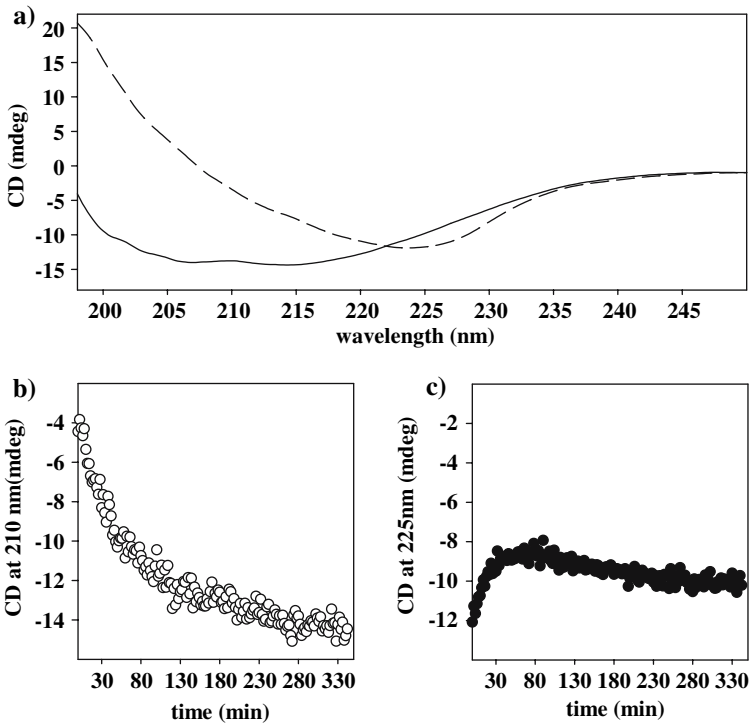

Fig. 4 **a** Far-UV CD spectra at 25°C of freshly prepared S-ConA sample at pH 8.9 (*dashed line*) and of the same sample after 300 min at 40°C (*continuous line*). Panels **b** and **c** show the time evolution of the CD signal at 210 and 225 nm, respectively, for S-ConA at pH 8.9 and at 40°C

axis). Both for S-ConA and ConA samples the kinetics of ANS emission well correlate with the kinetics of TT emission. This indicates a close relation between the tertiary structure conformational changes monitored by ANS fluorescence and the progress of amyloid fibrils formation. ANS emission is lower for S-ConA than for ConA, both before and after aggregation, indicating a more compact initial structure and a minor exposure of hydrophobic regions during the aggregation pathway.

Figure 4a reports the far-UV CD spectrum of a S-ConA sample at pH 8.9 after 300 min at 40°C (solid line) compared with the spectrum a of a freshly prepared sample at 25°C (dashed line). As observed for the native protein (Vetri et al. 2007), amyloid formation clearly involves extensive changes in the secondary structure of the protein. In Fig. 4b, c, the time evolution of the signal at 210 and 225 nm, respectively are reported. Data in panel b measured at 210 nm show that, as previously observed for ConA, the kinetic behaviour of the CD signal well correlates with the kinetics of TT and ANS fluorescence emission in the same conditions (Figs. 2, 3): there is a clear connection between secondary and tertiary structure changes and amyloid formation. The considerable change of the global shape of the far-UV spectrum during the aggregation pathway clearly indicates a large reorganization at secondary level to form new structures, such non-native β-aggregated structures, common in amyloid fibrils.

To further investigate the conformational changes involved in the fibrillation process, we also measured intrinsic tryptophans emission, which gives information on changes at the tertiary structure level (Militello et al. 2003). ConA intrinsic emission band is brought about by four tryptophans located in different sites of the monomer and, for this reason, it only gives mediate information on changes involving the regions where these residues are located. The time evolution of this signal at 40°C is reported in Fig. 5. Data shows that the emission intensity increases at the beginning of the kinetics as a function of time and, contemporary, a significant red-shift of the band occurs. Afterwards, the position of the band remains constant in the second part of the process. Emission spectra of tryptophans are widely used to monitor the solvent exposure degree of the chromophores and a red-shift of the bands indicates a more polar environment; moreover, their emission quantum yields may either decrease or increase upon the conformational changes in the surroundings (Vetri and Militello 2005; Souillac et al. 2003; Heegaard et al. 2005; Morel et al. 2006; Pedersen et al. 2006).

We report in Fig. 6 the behaviour of the moments (see ''Data Analysis'' section for further details) of the tryptophans emission band as a function of time. We observe an initial M_0 increase (Fig. 6a) for about 70 min, followed by a slow decay. M_1 (Fig. 6b) shows an initial red shift indicating a progressive more polar environment for tryptophans, and reaches a constant value after 70 min.

The characteristic times of M_0 and M_1 kinetics are faster than those observed for TT, ANS and CD signal at 210 nm. This suggests that some of the conformational changes at

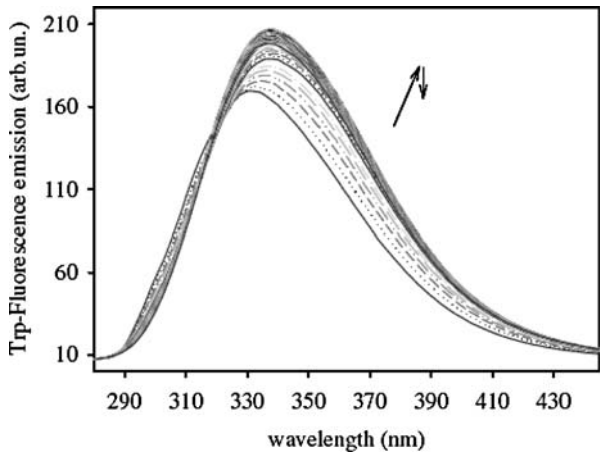

Fig. 5 Tryptophanil emission band for S-ConA at pH 8.9 and at 40°C at different times. The excitation wavelength was 270 nm. The *arrows* indicate the changes of the signals as a function of time

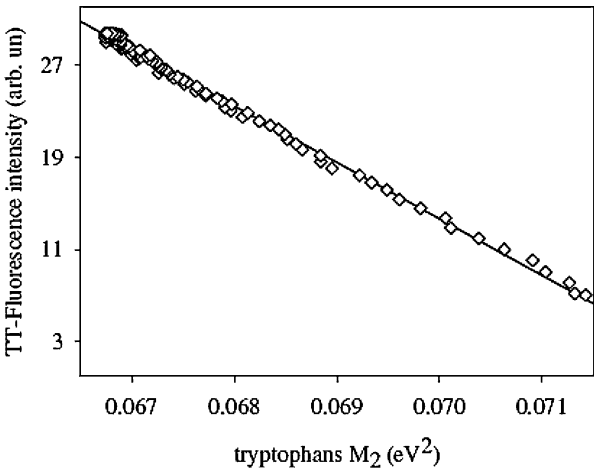

Fig. 7 TT fluorescence emission intensity as a function of the spectral moment M_2 of the tryptophanil emission band, in S-ConA sample at pH 8.9 and at 40°C

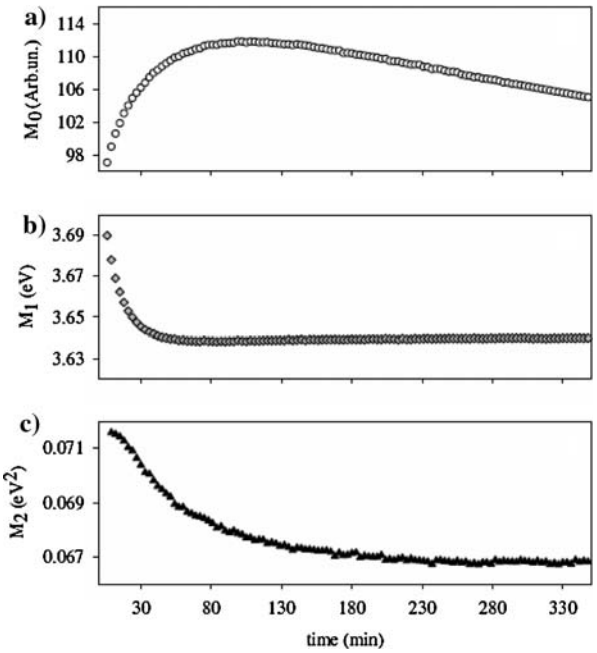

Fig. 6 Spectral moments M_0 (**a**), M_1 (**b**) and M_2 (**c**) of tryptophanil emission band for S-ConA at pH 8.9 and at 40°C as a function of time

the tertiary structure level precede, and probably drive, the aggregation process.

At difference from M_0 to M_1, M_2 shows a monotonic decay characterized by a longer evolution time (Fig. 6c). M_2 is essentially the broadening of the emission band, and can be related to protein conformational heterogeneity (Leone et al. 1999; Cupane et al. 1995). Therefore, the observed decrease is ascribable to changes in the tryptophans surroundings toward less heterogeneous structures. Interestingly, the kinetics of M_2 is characterized by a close correlation with the temporal evolution of TT emission as it can be seen in Fig. 7. Such correlation indicates that fibril formation reduces the conformational heterogeneity of protein molecules. In some instances, tryptophans emission properties, in particular the intensity and the average frequency, have been used as a conformational probe to assess solvent exposure during amyloid fibril formation, and a correlation between TT and tryptophan emission has been observed (Souillac et al. 2003; Heegaard et al. 2005; Morel et al. 2006; Pedersen et al. 2006). However, the signal of these intrinsic chromophores is not expected to distinguish between ordered fibrils and amorphous aggregates. In our conditions, the progressive ordering brought about by amyloid formation is clearly revealed by the correlation between TT fluorescence intensity and the second moment of tryptophans emission.

So far, we have shown that at pH 8.9 S-ConA and ConA seem to undergo similar fibrillation processes, even if with sizably different characteristic times and energy values.

As reported in the Introduction, ConA is widely used in medical applications (Tiegs et al. 1992; Ohta and Sitkovsky 2001; Song et al. 2003; Moreno et al. 2005; Fukuda et al. 2005); further, it has been reported to be able to induce programmed cell death in cortical neurons, by a mechanism involving the cross-linking of cell surface receptors, and with remarkable analogies with Programmed Cell Death induced by the amyloid β-peptide (Cribbs et al. 1996; Anderson et al. 1995). On the contrary, S-ConA was found to be unable to induce Programmed Cell Death (Cribbs et al. 1996). In view of these considerations, we investigated the propensity to form amyloid fibrils at physiological conditions (pH 7.2), both for ConA and S-ConA.

Figure 8 shows the elastic scattering (a) and TT emission (b) relative to ConA and S-Con A samples at pH 7.2 monitored during a temperature ramp at 12°C/h.

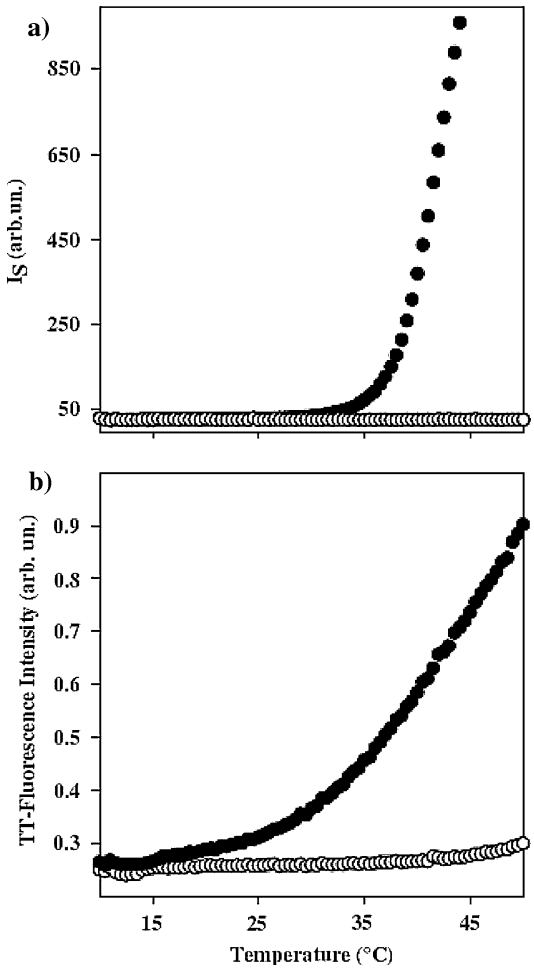

Fig. 8 **a** Elastic scattering intensity at $\lambda = 440$ nm, and **b** TT fluorescence emission (excitation wavelength 440 nm), as a function of temperature for ConA (*full symbols*) and S-ConA (*open symbols*). Both samples are at pH 7.2 and the scan rate is 12°C/h. Elastic scattering is measured on the excitation light of TT fluorescence, thus, data in the two panels are obtained in a single experiment

For Con A sample, elastic scattering remains constant and TT emission remains vanishing until 33°C, afterwards both values begin to increase. Signals relative to S-Con A sample do not show any relevant variation. Figure 9 shows the isothermal time evolution of TT emission intensity in ConA and S-ConA samples at 37°C and pH 7.2. Data reported in Figs. 8 and 9 clearly show that at neutral pH and at physiological temperatures ConA maintains a significant ability to form amyloid fibrils, while S-Con A does not.

Discussion

The mechanisms leading to protein aggregation and in particular to amyloid fibrils formation are the focus of extensive research. It is now commonly accepted that amyloid formation arises from at least partially unfolded

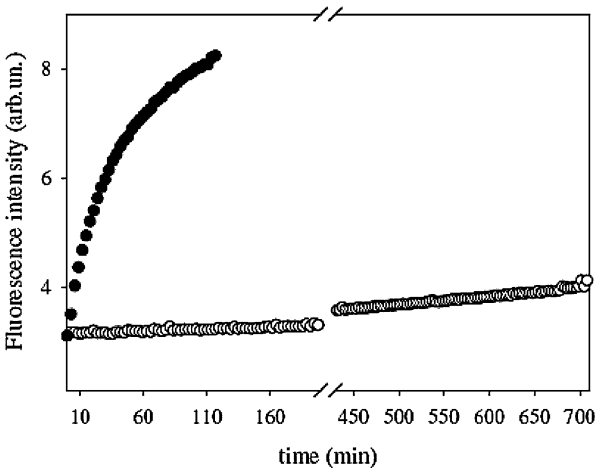

Fig. 9 TT fluorescence emission intensity, as a function of time, for ConA (*full symbols*) and S-ConA (*open symbols*) at pH 7.2 and at 37°C

structures (Uversky and Fink 2004); thus, conformational flexibility and solvent accessibility to key regions in protein structure are important factors in prompting fibrillation.

We found that both ConA and S-ConA present the ability to form fibrils. In both cases, the fibrillation process is favoured by alkaline pH, far from the isoelectric point of the protein, and strongly depends on temperature.

The experimental methods used to characterize the aggregation pathway allow us to separate different features involved in fibrils formation. For both proteins, a close correlation was observed between the progress of the fibrillation process and protein conformational changes, both at secondary and tertiary structural levels. Interestingly, the narrowing of tryptophan emission bands (as can be seen by the decreasing of M_2 values as a function of time) indicates a loss of heterogeneity in protein conformations, which perfectly correlates with fibrils formation (Fig. 7). Proteins are known to exist in a very large number of slightly different conformational substates. (see, e.g. Frauenfelder et al. 1988; Melchers et al. 1996; Cupane et al. 2003). Data shown in Fig. 7 suggest that in the ''amyloidal state'' protein molecules are characterized by a reduced number of conformational substates, with respect to the normally folded proteins. This observation claims for further investigations.

A comparison between results obtained for ConA and S-ConA samples suggests that the slower pathway observed for S-ConA fibrils can lead to more rigid and compact fibrils. This hypothesis seems to be confirmed by ANS emission measurement and reduction of M_2 relative to tryptophanil band.

The fact that the S-ConA results to be more stable and less prone to fibril formation (particularly at physiological

conditions, where essentially it does not aggregate) suggests that amyloid formation, together with the binding properties of the protein, may be an important factor for the ability of ConA to induce Programmed Cell Death in cortical neurons. In fact, S-ConA, which also binds to neurons surface, has been shown to not be able to induce Programmed Cell Death (Anderson et al. 1995; Cribbs et al. 1996). This suggestion needs to be investigated by means of suitable experiments on living cells. Furthermore, the significant ConA propensity to form amyloid fibrils at physiological conditions may constitute a serious experimental warning in all biomedical applications of the protein (Tiegs et al. 1992; Ohta and Sitkovsky 2001; Song et al. 2003; Moreno et al. 2005; Fukuda et al. 2005).

References

Anderson AJ, Pike CJ, Cotman CW (1995) Differential induction of immediate early gene proteins in cultured neurons by beta-amyloid (Aβ): association of c-jun with Aβ-induced apoptosis. J Neurochem 65:1487–1498

Bauer R, Carrotta R, Rischel C, Ogendal L (2000) Characterization and isolation of intermediates in b-Lactoglobulin heat aggregation at High pH. Biophys J 79:1030–1038

Bellotti V, Mangione P, Merlini G (2000) Immunoglobulin light chain amyloidoses. The archetype of structural and pathogenic variability. J Struct Biol 130:280–289

Bhattacharyya L, Koenig SH, Brown RD, Brewer CF (1991) Interactions of asparagines linked carbohydrates with Concanavalin A. Nuclear magnetic relaxation dispersion and circular dichroism studies. J Biol Chem 266:9835–9840

Chapman AL, Winterbourn CC, Brennan SO, Jordan TW, Kettle AJ (2003) Characterization of non-covalent oligomers of proteins treated with hypochlorous acid. Biochem J 375:33–40

Chatterjee A, Mandal DK (2005) Quaternary association and reactivation of dimeric Concanavalin A. Int J Biol Macromol 35:103–109

Collinge J (2001) Prion diseases of humans and animals: their causes and molecular basis. Annu Rev Neurosci 24:519–550

Cribbs DH, Kreng VM, Anderson J, Cotman CW (1996) Cross-linking of Concanavalin receptors on cortical neurons induces programmed cell death. Neuroscience 75:173–185

Cupane A, Leone M, Vitrano E, Cordone L (1995) Low temperature optical absorption spectroscopy: an approach to the study of stereodynamic properties of hemoprotein. Eur Biophys J 23:385–398

Cupane A, Militello V, Leone M (2003) Conformational substates and dynamic properties of carbonmonoxy hemoglobin. Biophys Chem 104:335–344

Dam TK, Roy R, Das SK, Oscarson A, Brewer CF (2000) Binding of multivalent carbohydrates to Concanavalin A and Dioclea Grandiflora lectin. J Biol Chem 275:14233–14230

Dam TK, Roy R, Page D, Brewer CF (2002a) Negative cooperativity associated with binding of multivalent carbohydrates to lectins. Thermodynamic analysis of the ''multivalency effect''. Biochemistry 41:1351–1358

Dam TK, Roy R, Page D, Brewer CF (2002b) Thermodynamic binding parameters of individual epitopes of multivalent carbohydrates to Concanavalin A as determined by ''reverse'' isothermal titration microcalorimetry. Biochemistry 41:1359–1363

Edelman GM (1972) Antibody structure and molecular immunology, Nobel Lecture

Emsley J, White HE, O'Hara BP, Oliva G, Srinivasan N, Tickle IJ, Blundell TL, Pepys MB, Wood SP(1994) Structure of pentameric human serum amyloid P component. Nature 367:338–345

Fatima S, Ahmad B, Khan RH (2006) Fluoroalcohols induced unfolding of Succinylated Con A: native like beta-structure in partially folded intermediate and alpha-helix in molten globule like state. Arch Biochem Biophys 454:170–180

Frauenfelder H, Parak F, Young RD (1988) Conformational substates in proteins. Annu Rev Biophys Biophys Chem 17:451–479

Fukuda T, Mogami A, Hisadome M, Komatsu H (2005) Therapeutic administration of Y-40138, a multiple cytokine modulator, inhibits Concanavalin A-induced hepatitis in mice. Eur J Pharmacol 523:137–142

Gunther GR, Wang JL, Yahara I, Cunningham BA, Edelman GM (1973) Concanavalin A derivatives with altered biological activities. Proc Natl Acad Sci USA 70:1012–1016

Hardman KD, Agarwal RC, Freiser MJ (1982) Manganese and calcium binding sites of Concanavalin A. J Mol Biol 5:69–86

Harper JD, Lansbury PT (1997) Models of amyloid seeding in Alzheimer's disease and scrapie: Mechanistic truths and physiological consequences of the time-dependent solubility of amyloid proteins. Annu Rev Biochem 66:385–407

Heegaard NH, Jorgensen TJ, Rozlosnik N, Corlin DB, Pedersen JS, Tempesta AG, Roepstorff P, Bauer R, Nissen MH (2005) Unfolding, aggregation, and seeded amyloid formation of lysine-58-cleaved beta 2-microglobulin. Biochemistry 44:4397–4407

Kelly JW (1998) The alternative conformations of amyloidogenic proteins and their multi-step assembly pathways. Curr Opin Struc Biol 8:101–106

Lakovicz JR (1983) Principles of fluorescence spectroscopy. Plenum Press, New York

Leone M, Agnello S, Boscaino R, Cannas M, Gelardi FM (1999) Conformational disorder in vitreous systems probed by photoluminescence activity in SiO2. Phys Rev B 60:11475–11481

Librizzi F, Rischel C (2005) The kinetic behavior of insulin fibrillation is determined by heterogeneous nucleation pathways. Protein Sci 14:3129–3134

Mangold SL, Cloninger MJ (2006) Binding of monomeric and dimeric Concanavalin A to mannose-functionalized dendrimers. Org Biomol Chem 4:2458–2465

Melchers B, Knapp EW, Parak F, Cordone L, Cupane A, Leone M (1996) Structural fluctuation of Myoglobin from normal-modes, Mössbauer, Raman, and absorption spectroscopy. Biophys J 70:2092–2099

Militello V, Vetri V, Leone M (2003) Conformational changes involved in thermal aggregation processes of Bovine Serum Albumin. Biophys Chem 105:133–141

Mitra N, Srinivas VR, Ramya TNC, Ahmad N, Reddy GB, Surolia A (2002) Conformational stability of legume lectins reflect their different modes of quaternary association: solvent denaturation studies on Concanavalin A and winged bean acidic agglutin. Biochemistry 41:9256–9263

Moothoo DN, McMahon SA, Dimick SM, Toone EJ, Naismith JH (1998) Crystallization of succinylated Concanavalin A bound to a synthetic bivalent ligand and preliminary structural analysis. Acta Crystallogr D Biol Crystallogr 54:1023–1025

Morel B, Casare S, Conejero-Lara F (2006) A single mutation induces amyloid aggregation in the alpha-spectrin SH3 domain: analysis of the early stages of fibril formation. J Mol Biol 356:453–468

Moreno C, Gustot T, Nicaise C, Quertinmont E, Nagy N, Parmentier M, Le Moine O, Deviere J, Louis H (2005) CCR5 deficiency exacerbates T-cell-mediated hepatitis in mice. Hepatology 42:854–862

Naiki H, Gejyo F (1999) Kinetic analysis of amyloid fibril formation. Methods Enzymol 309:305–318

Naiki H, Higuchi K, Hosokawa M, Takeda T (1989) Fluorometric determination of amyloid fibrils in vitro using the fluorescent dye, thioflavine T. Anal Biochem 177:244–249

Ohta A, Sitkovsky M (2001) Role of G-protein-coupled adenosine receptors in down regulation of inflammation and protection from tissue damage. Nature 414:916–920

Pedersen JS, Dikov D, Flink JL, Hjuler HA, Christiansen G, Otzen DE (2006) The changing face of glucagon fibrillation: structural polymorphism and conformational imprinting. J Mol Biol 355:501–523

Relini A, Canale C, Torrassa S, Rolandi R, Ghiozzi A, Rosano C, Bolognesi M, Plakoutsi G, Bucciantini G, Chiti F, Stefani M (2004) Monitoring the process of HypF fibrillization and liposome permeabilization by protofibrils. J Mol Biol 338:943–957

Rochet C, Lansbury PT (2000) Amyloid fibrillogenesis: themes and variations. Curr Opin Struct Biol 10:60–68

Sanders JN, Chenoweth SA, Schwarz FP (1998) Effect of metal ion substitutions in Concanavalin A on the binding of carbohydrates and on thermal stability. J Inorg Biochem 70:71–82

Senear DF, Teller DC (1981) Effects of saccharide and salt binding on dimer-tetramer equilibrium of Concanavalin A. Biochemistry 20:3076–3083

Sinha S, Mitra N, Kumar G, Bajaj K, Surolia A (2005) Unfolding studies on soybean Agglutinin and Concanavalin A tetramers: a comparative account. Biophys J 88:1300–1310

Song E, Lee SK, Wang J, Ince N, Ouyang N, Min J, Chen J, Shankar P, Lieberman J (2003) RNA interference targeting Fas protects mice from fulminant hepatitis. Nat Med 9:347–351

Souillac PO, Uversky VN, Fink AL (2003) Structural transformations of oligomeric intermediates in the fibrillation of the immunoglobulin light chain LEN. Biochemistry 42:8094–8104

Tiegs G, Hentschel J, Wendel A (1992) A T cell-dependent experimental liver injury in mice inducible by Concanavalin A. J Clin Invest 90:196–203

Uversky WN, Fink AL (2004) Conformational constraints for amyloid fibrillation: the importance of being unfolded. Biochim Biophys Acta 1698:131–153

Vetri V, Militello V (2005) Thermal induced conformational changes involved in the aggregation pathways of beta-lactoglobulin. Biophys Chem 113:83–91

Vetri V, Canale C, Relini A, Librizzi F, Militello V, Ghiozzi A, Leone M (2007) Amyloid fibrils formation and amorphous aggregation in Concanavalin A. Biophys Chem 125:184–190

Vivian JT, Callis PR (2001) Mechanisms of tryptophan fluorescence shifts in proteins. Biophys J 80:2093–2109

Waner MJ, Gilchrist M, Schindler M, Dantus M (1998) Imaging the molecular dimensions and oligomerization of proteins R liquid/solid interfaces. J Phys Chem B 102:1649–1657